ELSEVIER

Materials Science and Engineering A250 (1998) 270–278

MATERIALS SCIENCE & ENGINEERING A

On the matrix cracking stress and the redistribution of internal stresses in brittle-matrix composites

Edgar Lara-Curzio *, Christiana M. Russ

Metals and Ceramics Division, Oak Ridge National Laboratory, Oak Ridge, TN 37831-6069, USA

Abstract

A concept is proposed to increase the matrix cracking stress of some brittle-matrix composites by taking advantage of the redistribution of internal stresses that occurs when a composite with phases that have dissimilar creep behavior is subjected to thermomechanical loading. The concept is elaborated through the stress analysis of a model unidirectional composite with constituents that exhibit linear viscoelastic behavior. It is shown that if a composite with a matrix that is less creep resistant than the fibers is subjected to a treatment involving both thermal and mechanical loading (e.g. creep test), stresses can be transferred from the matrix to the fibers, resulting in the stress–relaxation of the matrix. Furthermore, it is also shown that by the elastic recovery of the fibers, the matrix can be subjected to large compressive residual stresses at the end of the treatment. The conditions for the viability of this concept and the implications of fiber overloading and potential loss of composite-like behavior are discussed.

Keywords: Brittle-matrix; Composites; Cracking stress; Internal stress

1. Introduction

The driving force behind the development of continuous fiber-reinforced ceramic composites (CFCCs) is the promise of substantial economic and environmental benefits if they are used in defense, energy and related industrial technologies, particularly at elevated temperatures [1]. The main attraction for using CFCCs over other high temperature materials, particularly monolithic ceramics, is their superior toughness, tolerance to the presence of cracks and non-catastrophic mode of failure. The mechanisms responsible for the tough behavior of CFCCs are based on the ability of the reinforcing fibers to bridge matrix cracks by fiber debonding and sliding. These mechanisms are often aided by the presence of fiber coatings that form low toughness interfaces between the fiber, the fiber coating, and the matrix, and an appropriate state of residual stresses in the fiber-matrix interfacial zone.

In contrast to the linear elastic stress–strain behavior that monolithic ceramics exhibit when loaded in tension, CFCCs typically exhibit non-linear behavior at stresses above the so-called proportional stress limit, σ_{mc}, due mainly to progressive matrix cracking, fiber debonding and fiber sliding (Fig. 1). Although matrix cracking above σ_{mc} reduces the stiffness of the composite, matrix microcracks do form at stresses below σ_{mc} without detectable changes in the specimen compliance [2]. Because most of the applications for which CFCCs are being considered involve aggressive envi-

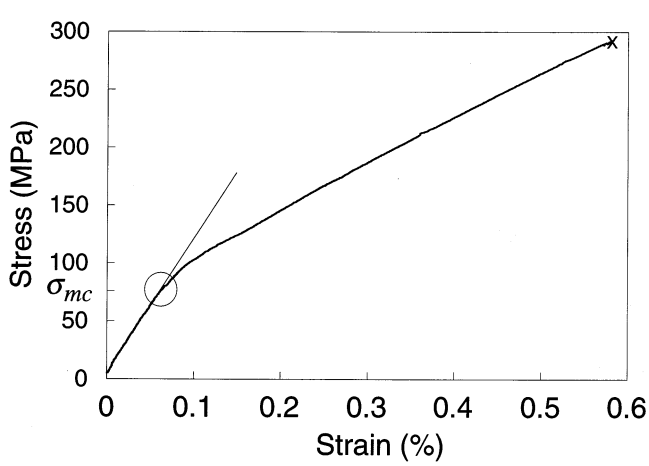

Fig. 1. Typical stress–strain curve exhibited by a CFCC under monotonic tensile loading.

* Corresponding author. Tel. +1 423 5741749; fax: +1 423 5746098; e-mail: laracurzioe@ornl.gov

0921-5093/98/$19.00
PII S0921-5093(98)00601-7

ronments [1], matrix cracks will invariably allow the ingress of the environment into the composite, resulting in the degradation of the fiber coating and the fibers, and eventually in loss of strength and failure. It is often found that σ_{mc} is the threshold stress for the occurrence of delayed failure during stress-rupture or mechanical cyclic fatigue testing (Ref. [3,4]). Therefore, in the absence of environmentally stable fibers and fiber coatings, the matrix cracking stress is currently being considered a safe design limit for CFCCs.

Due to the difficulty in synthesizing fully dense and defect-free matrices, the value of the matrix cracking stress for many 2-D CFCCs is relatively low (typically < 100 MPa), a fact that will certainly limit their use to low-stress applications. This realization has prompted efforts in the composites community to devise means for increasing the matrix cracking stress of CFCCs. A lower bound to the matrix cracking stress for a unidirectional CFCC, σ_{mc}, is given by [5]

$$\bar{\sigma}_{mc} = E_c \sqrt[3]{\frac{6\tau\Gamma_m f^2 E_f}{(1-f)E_m^2 r E_c}} - \sigma^T \quad (1)$$

where τ is the interfacial shear stress, Γ_m is the matrix fracture energy, f the fiber volume fraction, E_f, E_m, and E_c are Young's moduli for the fibers, matrix, and composite, respectively, r is the fiber radius, and σ^T is the misfit stress, which is a measure of the axial residual stress in the matrix [5]. Although the magnitude of the matrix cracking stress can be modified by changing the properties of the constituents, their concentration, or the nature of the fiber–matrix interface as indicated by Eq. (1), the largest effect on the magnitude of the matrix cracking stress can be realized by modifying the axial residual stress in the matrix.

The idea of increasing the matrix cracking stress by modifying the state of residual stresses in composites is not new. Perhaps the best known case of the application of this concept is pre-stressed concrete. Pre-stressed concrete is obtained by casting the concrete around the reinforcing bars which are placed under tension between permanent anchors at the ends of the casting bed. When the concrete reaches its desired strength, the ends of the pre-stressing wires are cut off, placing the concrete elements under compression by the elastic recovery of the reinforcing wires [6].

Although pre-stressing the reinforcing fibers during the fabrication of CFCCs is not practical, the state of residual stresses in composites can also be modified by taking advantage of redistribution of internal stresses that takes place during composite creep, especially when the composite constituents have dissimilar creep resistance. The potential of this concept had already been identified [7], but in this paper, this concept is modeled through the stress analysis of a unidirectional model composite with linear viscoelastic constituents, that is subjected to both thermal and mechanical loading (e.g. creep loading conditions).

Related evidence of the relationship between the redistribution of internal stresses in composites and the occurrence of matrix cracking was documented during the creep evaluation of SiC/Si_3N_4 composites at 1200°C in air [8]. It was found that both the shape of the creep strain versus time curves and the life of the specimen depended strongly on the rate of mechanical loading up to the creep test stress. By loading the specimens at a rate of 0.25 MPa s^{-1} up to the test stress of 250 MPa, the specimens exhibited typical creep behavior and had lives of about 110 h. On the other hand, when the specimens were loaded at a faster rate of 100 MPa s^{-1}, the shape of the creep strain versus time curves were quite different and the lives of the specimens were found to be three orders of magnitude shorter. The explanation of these observations, which is supported by the predictions of the model presented in this paper, was that loading the specimen at a slow rate allowed sufficient time for stress relaxation of the matrix during mechanical loading, thus avoiding matrix cracking [8]. On the other hand, at rapid loading rates, there was not enough time to allow for the stress relaxation of the matrix, resulting in matrix cracking that ultimately led to the oxidation of the fibers and rapid composite failure.

The creep behavior of composites has been modeled by several; Holmes et al. have conducted a good review of this work [9]. Existent models differ in complexity, from simple 1-D models of unidirectional composite with elastic fibers embedded in a creeping matrix, to more complex 2-D and 3-D finite-element stress analysis. In most of these modeling efforts, the constitutive behavior of the composite constituents have been described using empirical equations of the Norton-type [9]. The parameters for these equations, which relate the stress to the rate of deformation during the so-called 'steady state creep regime', are typically obtained from constant-stress creep experiments. However, as shown below and elsewhere [9], the use of this type of empirical equations, which are derived from constant stress experiments is questioned because the stress acting on the phases of a composite that exhibit dissimilar creep behavior during a creep test is not constant. A simple but detailed analysis of the type of errors which can occur through use of inappropriate constitutive equations to model the behavior of the composite constituents has been reported elsewhere [10].

Scherer and Rekhson obtained analytical solutions to predict the structural relaxation in several composite systems with viscoelastic phases [11]. Their stress analysis of an elastic core surrounded by a glass cladding, involved use of the correspondence principle or elastic–viscoelastic analogy, which converts a viscoelastic stress

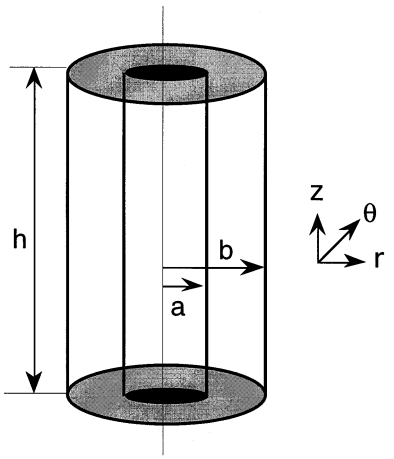

Fig. 2. Geometric representation of model unidirectional composite.

analysis into an equivalent elastic problem by making use of Laplace transform techniques [12]. An adaptation of this elastic–viscoelastic analogy is used in the present paper in solving the problem of the stress analysis of a unidirectional model composite with linear viscoelastic phases so as to determine the evolution of internal stresses when such composite is subjected to simultaneous thermal and mechanical loading. The general implications of the model predictions are discussed in relation to the practical aspects of the proposed concept to increase the matrix cracking stress of some brittle-matrix composites.

2. Model

2.1. Stress analysis

The geometry of the system of interest is idealized in Fig. 2. It consists of an arrangement of two long concentric cylinders representing a cylindrical fiber embedded in a cylindrical shell with the properties of the matrix. Because of the axisymmetric nature of the problem, the circumferential component of the displacements is zero, and by assuming that $h/b >> 1$, end-effects can be neglected so that plane strain conditions prevail (planes normal to the axis of the cylinder remain planar as stresses develop), i.e.

$$\varepsilon_z^{\mathrm{f}} = \varepsilon_z^{\mathrm{m}} \tag{2}$$

Hereafter, superscripts f and m refer to the fiber and the matrix, respectively, while r, θ, and z are associated with the cylindrical coordinates (Fig. 2).

Equilibrium of forces in a cylindrical differential element result in

$$\sigma_r = \frac{\mathrm{d}}{\mathrm{d}r}(r\sigma_\theta) \tag{3}$$

and

$$\sigma_\theta = \frac{\mathrm{d}}{\mathrm{d}r}(r\sigma_r) \tag{4}$$

which combined yield solutions of the form:

$$\sigma_r = A - \frac{B}{r^2} \tag{5}$$

and

$$\sigma_\theta = A + \frac{B}{r^2} \tag{6}$$

where A and B are integration constants that have different values for each of the two phases in the model composite shown in Fig. 2. The boundary conditions require continuity of tractions at the fiber–matrix interface (i.e. $r = a$) and zero-normal forces acting on the free surface, i. e.

$$\sigma_r^{\mathrm{f}}(r = a) = \sigma_r^{\mathrm{m}}(r = a)$$

and

$$\sigma_r^{\mathrm{m}}(r = b) = 0$$

Upon enforcement of the boundary conditions, the unknown constants A and B in Eqs. (5) and (6) can be eliminated, as applied to each phase, in favor of the still unknown interfacial normal stress, P:

$$\sigma_r^{\mathrm{f}} = \sigma_\theta^{\mathrm{f}} = -P \tag{7}$$

$$\sigma_r^{\mathrm{m}} = \frac{fP}{1-f}\left(1 - \frac{b^2}{r^2}\right) \tag{8}$$

$$\sigma_\theta^{\mathrm{m}} = \frac{fP}{1-f}\left(1 + \frac{b^2}{r^2}\right) \tag{9}$$

where f is the fiber volume fraction, i.e.

$$f = \frac{a^2}{b^2}$$

A balance of forces in the axial direction results in the so-called rule of mixtures

$$f\sigma_z^{\mathrm{f}} + (1-f)\sigma_z^{\mathrm{m}} = \sigma_{\mathrm{c}} \tag{10}$$

where σ_{c} is the stress applied to the composite in the axial direction.

By assuming that the fiber is bonded to the matrix, continuity of radial displacements at the fiber–matrix interface requires that

$$\varepsilon_\theta^{\mathrm{f}}(r = a) = \varepsilon_\theta^{\mathrm{m}}(r = a) \tag{11}$$

Eqs. (2) and (11) are the 'composite' equations, which can be solved simultaneously once the constitutive behaviors (stress–strain relationships) are prescribed. The solution to the problem is given by finding the unknown normal interfacial stress, P, and the axial stress in the fiber, σ_z^{f}.

2.2. Constitutive relations

The constitutive relationship for a material that exhibits linear viscoelastic behavior in a state of multiaxial stress–multiaxial strain, has the following form:

$$\varepsilon_{ij} = \frac{\bar{H}_1}{\bar{Q}_1}\sigma_{ij} - \frac{\bar{H}_2\bar{Q}_1 - \bar{H}_1\bar{Q}_2}{3\bar{Q}_1\bar{Q}_2}\sigma_{kk}\delta_{ij} + \alpha\Delta T\delta_{ij} \quad (12)$$

where $\bar{H}_i$ and $\bar{Q}_i$ are linear operators of the form:

$$\bar{H}_1 s_{ij} = \bar{Q}_1 e_{ij} \quad (13)$$

$$\bar{H}_2\sigma_{kk} = \bar{Q}_2\varepsilon_{kk} \quad (14)$$

s_{ij} and e_{ij} are the deviatoric stress and strain tensors, σ_{kk} and ε_{kk} the traces of the stress and strain tensors, α is the linear coefficient of thermal expansion, ΔT is the change in temperature from the stress-free reference temperature and δ_{ij} is Kronecker's delta.

Note that Eq. (12) has been written in such a general form that it is reduced to the well known Hooke's law when the operators are replaced as follows

$$\bar{H}_1 = 1 \quad (15)$$

$$\bar{H}_2 = 1 \quad (16)$$

$$\bar{Q}_1 = 2G \quad (17)$$

$$\bar{Q}_2 = 3K \quad (18)$$

where G and K are the elastic shear and bulk moduli, respectively. Because of the different behavior of viscoelastic materials to shear and dilation, and because we often deal with extensional strains that change both the shape and the volume of a body, it is advantageous to separate the hydrostatic and deviatoric components of the stress and the strain.

2.3. Thermoelastic stress problem

Before solving the viscoelastic stress problem, the associated thermoelastic stress problem will be addressed. The thermoelastic stress problem happens to be the time-independent version of the viscoelastic stress problem and provides the initial conditions for the solution of the latter. The solution to the thermoelastic stress problem is obtained by solving simultaneously the composite equations (Eqs. (2) and (11)) using the general constitutive equation (Eq. (12)) with the time-independent operators (Eqs. (15)–(18)), assuming $\sigma_c = 0$ and the appropriate change in temperature, ΔT, from the original stress-free fabrication temperature to the treatment temperature. In this analysis, it will be assumed that the material properties are temperature-independent, and that changes in temperature occur instantaneously, so that they only induce elastic residual stresses. Substitution of Eq. (12),and Eqs. (15)–(18) into Eqs. (2) and (11) yield:

Table 1
Numerical values used in the calculations

G_f	8.33×10^{10} Pa
K_f	1.11×10^{11} Pa
G_m	3.85×10^{10} Pa
K_m	8.33×10^{10} Pa
α^f	4×10^{-6}/°C
α^m	5×10^{-6}/°C
R_2	2.0×10^{10} Pa
η_1	1×10^{14} Pa s^{-1}
η_2	2×10^{12} Pa s^{-1}
T_1	1000°C
T_2	500°C
T_3	20°C

$$[\Psi]\begin{bmatrix} P \\ \sigma_z^f \end{bmatrix} = [\Omega] \quad (19)$$

where the matrix Ψ and vector Ω contain terms associated with the system geometry, material properties and thermal and mechanical loading conditions.

Let us consider the state of residual stresses of the model composite, idealized by the system of concentric cylinders in Fig. 2, at a temperature T_2 that is different from the fabrication temperature T_1, $(T_2 < T_1)$. Further, let us assume that the composite constituents possess the properties summarized in Table 1. After solving the system of simultaneous equations in Eq. (19) for P, and σ_z^f, Fig. 3 shows the predicted axial and normal residual stresses in the fiber and matrix, per degree of cooling, as a function of the fiber concentration, f. Notice that because $\alpha^m > \alpha^f$, and $T_2 < T_1$, the fibers are under radial compression and the matrix in axial tension, which is typical of many composite systems of interest (e. g. Nicalon™/CAS, Nicalon™/BMAS). In these cases, fiber radial compression is desirable to promote friction during fiber sliding.

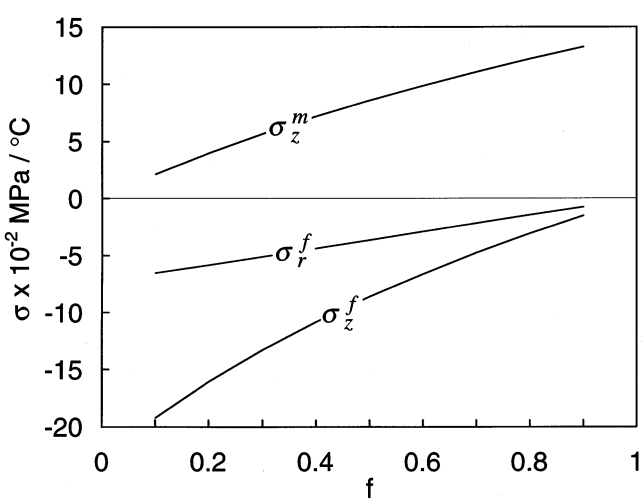

Fig. 3. Residual stresses in model unidirectional composite as a function of the concentration of fibers. The stresses are given per degree of cooling from the stress-free fabrication temperature. The material properties in Table 1 were used in the calculations.

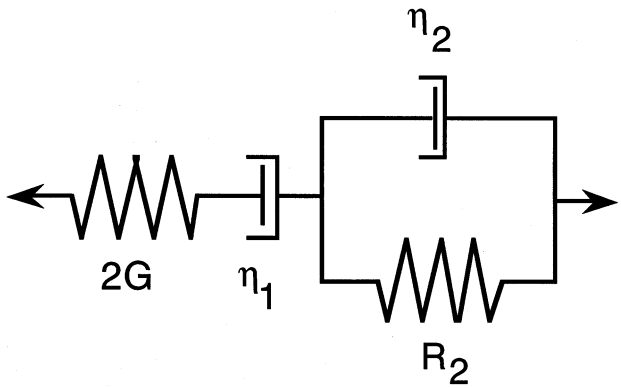

Fig. 4. Schematic representation of the Burgers material model. It consists of a Maxwell element in series with a Kelvin-Voigt element. This material model was used to describe the behavior of the matrix under distortion.

2.4. Viscoelastic stress problem.

In order to solve the viscoelastic stress problem, it is necessary to prescribe first the constitutive behavior of the composite phases. There is an infinite number of viscoelastic material models and their complexity typically increases with their predictive power [13]. One of the simplest models, yet capable of predicting results that are qualitatively remarkably similar to the behavior of real materials is the Burgers material model. Fig. 4 shows its schematic representation. The Burgers material model consists of Maxwell and Kelvin-Voigt material model in series, which at the same time, are constructed using the basic units, spring and dash-pot, in series and in parallel, respectively [13]. Fig. 5 shows the response of a material that behaves elastically under dilation but as a Burgers material under distortion during a creep–creep recovery test. The time in Fig. 5 has been normalized by the retardation time of the

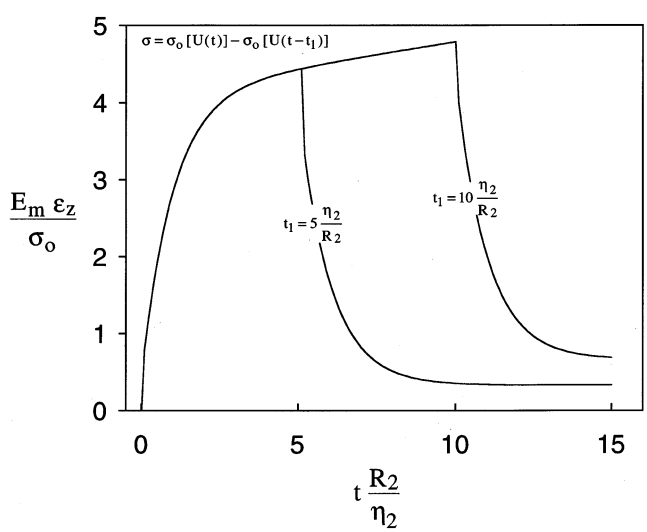

Fig. 5. Strain history exhibited by a material that is elastic under dilation but that behaves as a Burgers material under distortion, when subjected to a creep–creep recovery test.

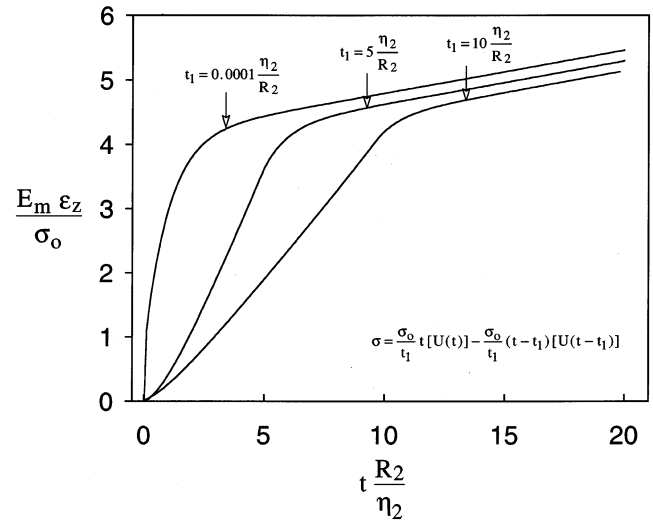

Fig. 6. Effect of the rate of loading up to the test stress, on the response of a material that is elastic under dilation but that behaves as a Burgers material under distortion, when subjected to a creep test.

Kelvin part of the Burgers model. Upon the sudden application of stress, this material model exhibits instantaneous recoverable strain, delayed elasticity and unrecoverable viscous deformation. Under creep loading conditions, for example, the delayed elastic response is a transient usually referred to as 'primary' creep, whereas the constant rate of deformation at longer times, associated with viscous deformation, is often referred to as 'steady state' creep. Upon the removal of stress, the material exhibits instantaneous recovery of the elastic strain, delayed strain recovery associated with the deformation of the Kelvin-Voigt part of the model, and permanent viscous deformation associated with the elongation of the dash-pot in the Maxwell part of the model.

Fig. 6 shows the effect of loading rate on the axial response of the same material. At slow loading rates, the strain exhibits a parabolic time dependence that is characteristic of many materials. In relation to the loading schedules in Figs. 5 and 6, $[U(x)]$ is Heaviside's unit function defined as

$$[U(x-x_0)] = 1 \quad x \geq x_0$$

$$[U(x-x_0)] = 0 \quad x < x_0$$

Without losing generality, the special case of an elastic fiber embedded in a matrix that behaves as a Burgers material under distortion and elastically under dilation will be considered. This choice was made because of the simplicity and realism of the Burgers material model. As such, the linear operators in Eq. (13) take the following form [13]

For the fiber:

$$\bar{H}_1^f = 1 \tag{20}$$

$$\bar{H}_2^f = 1 \tag{21}$$

$$\bar{Q}_1^{\mathrm{f}} = 2G_{\mathrm{f}} \tag{22}$$

$$\bar{Q}_2^{\mathrm{f}} = 3K_{\mathrm{f}} \tag{23}$$

For the matrix:

$$\bar{H}_1^{\mathrm{m}} = 1 + \left(\frac{\eta_1}{2G_{\mathrm{m}}} + \frac{\eta_1}{R_2} + \frac{\eta_2}{2G_{\mathrm{m}}}\right)\frac{\partial}{\partial t} + \frac{\eta_1\eta_2}{2G_{\mathrm{m}}R_2}\frac{\partial^2}{\partial t^2} \tag{24}$$

$$\bar{Q}_1^{\mathrm{m}} = \eta_1\frac{\partial}{\partial t} + \frac{\eta_1\eta_2}{R_2}\frac{\partial^2}{\partial t^2} \tag{25}$$

$$\bar{H}_2^{\mathrm{m}} = 1 \tag{26}$$

$$\bar{Q}_2^{\mathrm{m}} = 3K_{\mathrm{m}} \tag{27}$$

where K_{f}, K_{m}, G_{f}, and G_{m} are the elastic bulk and shear moduli for the fiber and matrix, respectively, and η_i and R_2 are the coefficients of viscosity and spring constant, respectively, for the Burgers model shown in Fig. 4.

By substituting the relationships between stress and strain (Eqs. (12) and (20)–(27)) into the composite equations (Eqs. (2) and (11)), a system of simultaneous differential equations (Eq. (28)) is obtained for the unknown interfacial normal stress and the fiber axial stress.

$$[\Phi_1]\begin{bmatrix}\ddot{P}\\ \ddot{\sigma}_z^{\mathrm{f}}\end{bmatrix} + [\Phi_2]\begin{bmatrix}\dot{P}\\ \dot{\sigma}_z^{\mathrm{f}}\end{bmatrix} + [\Phi_3]\begin{bmatrix}P\\ \sigma_z^{\mathrm{f}}\end{bmatrix} = [\Xi] \tag{28}$$

In Eq. (28) the matrices Φ_i, and the vector Ξ, contain terms associated with the model geometry, material properties, and the mechanical loading schedule.

Let us now consider the thermomechanical schedule shown in Fig. 7. It consists of 'instantaneous' cooling from the fabrication temperature, T_1, to the treatment temperature T_2, at time zero. Afterwards, temperature is kept constant until time t_2, when the temperature is reduced again 'instantaneously' from the treatment temperature T_2, to the service temperature T_3. Starting also at time zero, the specimen is stressed in the axial direction at a constant loading rate up to the treatment stress σ_0. The rate of mechanical loading may be varied by changing the value of t_1 in relation to the schedule in Fig. 7. Once the applied composite stress reaches σ_0, at time t_1, it is kept constant afterwards until time t_2, when it is removed 'instantaneously' at the same time that the specimen is cooled from T_2 down to T_3. Mathematically the thermal and mechanical loading schedules are described as follows:

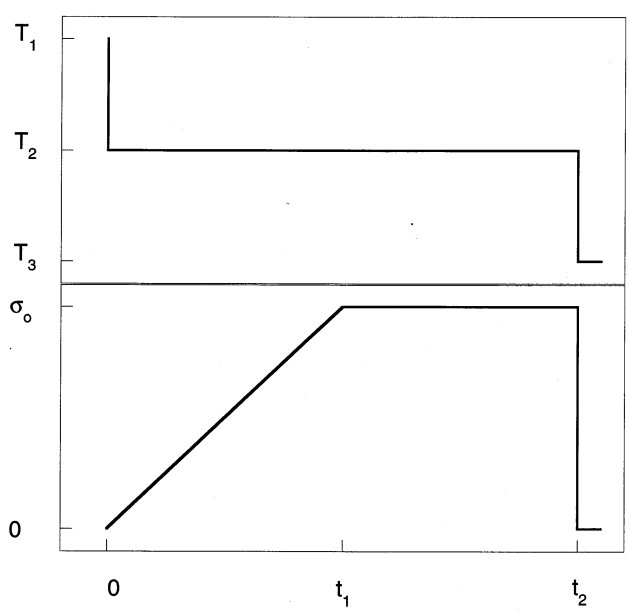

Fig. 7. Thermomechanical schedule used to promote the redistribution of internal stresses in model composite.

$$T = T_1 + (T_2 - T_1)[U(t)] + (T_3 - T_2)[U(t - t_2)]$$

$$\sigma_c = \frac{\sigma_0}{t_1}t[U(t)] - \frac{\sigma_0}{t_1}(t - t_1)[U(t - t_1)] - \sigma_0[U(t - t_2)]$$

In the previous section the state of residual stresses of the same composite material was calculated, and as it was indicated, the state of stress associated with a change in temperature of $(T_2 - T_1)$ degrees corresponds to the initial conditions for the viscoelastic problem. The solution to the viscoelastic stress analysis is obtained by solving the system of simultaneous linear differential equations in Eq. (28) for the thermomechanical schedule shown in Fig. 7 up to time t_2, and the initial conditions prescribed by the thermoelastic residual stress problem. At the end of the treatment, elastic stresses associated with instantaneous cooling from T_2 to T_3 and the instantaneous removal of the composite stress from σ_0 to 0, at time t_2, were superimposed to the stresses obtained from the viscoelastic problem.

3. Results

The effect of fiber concentration on the redistribution of internal stresses in the model composite was investigated first. Fig. 8 shows the evolution of the axial stress in the fiber, normalized by the applied composite stress, σ_0, for fiber volume fractions of 0.1, 0.3 and 0.5. The horizontal axis in Fig. 8 is the time normalized by the retardation time of the Kelvin-Voigt part of the Burgers material model that describes the behavior of the matrix under distortion. As it was already indicated, the value of the fiber axial stress at time zero is given by the thermoelastic problem for a temperature change of $(T_2 - T_1)$ degrees (Fig. 3). In Fig. 8 it can be observed that upon the application of the stress, the axial stress in the fiber rises rapidly, and once the composite stress reaches σ_0 and remains constant afterwards, the axial stress in the fiber increases non-linearly with time approaching an asymptotic value of σ_0/f at long times. At this point the fibers bear all the load.

When the load is removed suddenly at time t_2, at the same time that the specimen is cooled down from T_2 to

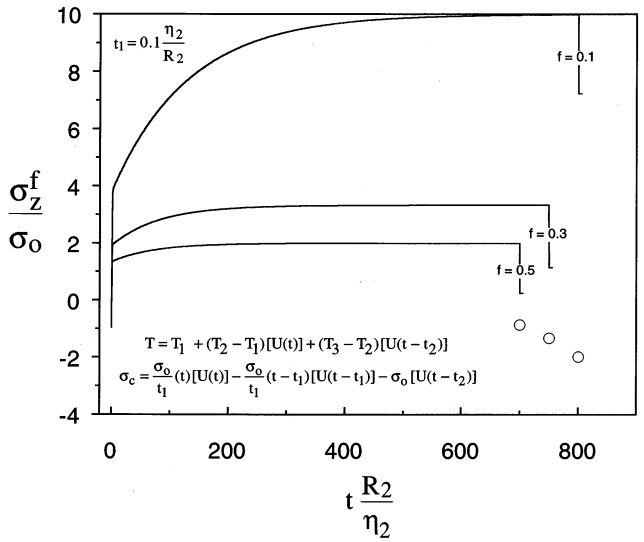

Fig. 8. Predicted evolution of the axial stress in the fiber when the model composite is subjected to the thermomechanical schedule shown in Fig. 7. The open circles indicate the state of residual stress that would exist in the fiber, if the composite had simply been cooled from the stress-free fabrication temperature, T_1, down to the service temperature, T_3. The model predictions are shown for three values of the fiber volume fraction.

T_3, the axial stress in the fibers drops to a level that can be considered the new state of residual stresses in the fiber at the service temperature T_3. This new residual stress level is contrasted with that that would exist in the fiber by simply cooling the composite from the fabrication temperature by $(T_3 - T_1)$ degrees, as indicated by the open circles in Fig. 8. The results in Fig. 8 clearly show that at the end of the thermomechanical treatment, the fiber is subjected to large tensile stresses, in contrast to the compressive stresses that would exist otherwise, and that the magnitude of the residual stress is inversely proportional to the fiber concentration.

By equilibrium considerations, the axial stress in the matrix is found using Eq. (10), and Fig. 9 shows the evolution of the axial stress in the matrix during the same treatment process. At time zero, the value of the axial stress in the matrix is obtained from the thermoelastic problem for a temperature change of $(T_2 - T_1)$ degrees from the stress-free fabrication temperature (Fig. 3). It can be observed that the axial stress in the matrix rises rapidly upon the application of the composite stress, but then decays towards zero after the stress in the composite reaches σ_0 and it is maintained constant thereafter. Upon simultaneous mechanical unloading and cooling of the composite to the service temperature T_3 at time t_2, the stress in the matrix becomes compressive, with magnitude that is inversely proportional to the fiber concentration. This new state of residual stresses is contrasted with the one that would exist if the specimen had been simply cooled from the original stress-free fabrication temperature T_1 down to the service temperature T_3, which is represented by the open circles. In other words, by means of the thermomechanical treatment described in Fig. 7, the state of residual stresses in the composite was substantially modified, and in the case of the matrix, it was changed advantageously from tensile to compressive. Thus, these results demonstrate the viability of the concept proposed here to increase the matrix cracking stress by subjecting the matrix to compressive stresses as a result of the redistribution of internal stresses that occurs in composites when subjected to creep, particularly when the phases exhibit dissimilar creep resistance.

It can be observed in Fig. 9 that at the end of the mechanical loading segment at time t_1, the stress in the matrix is a good fraction of the applied composite stress. The implications of this observation are clear in the context of this paper since matrix cracking could occur during mechanical loading if the axial stress in the matrix exceeded the matrix cracking stress. Fig. 10 shows the evolution of the axial stress in the matrix when the composite is loaded at a loading rate three orders of magnitude slower. It can be observed for the cases when $f = 0.1$, and $f = 0.3$ that the axial stress in the matrix decreases continuously even though the stress in the composite continues to increase up to time t_1. Fig. 11 specifically shows the effect of the mechanical loading rate on the evolution of the matrix axial stress during the treatment and just serves to reinforce the observations already made. These model predictions

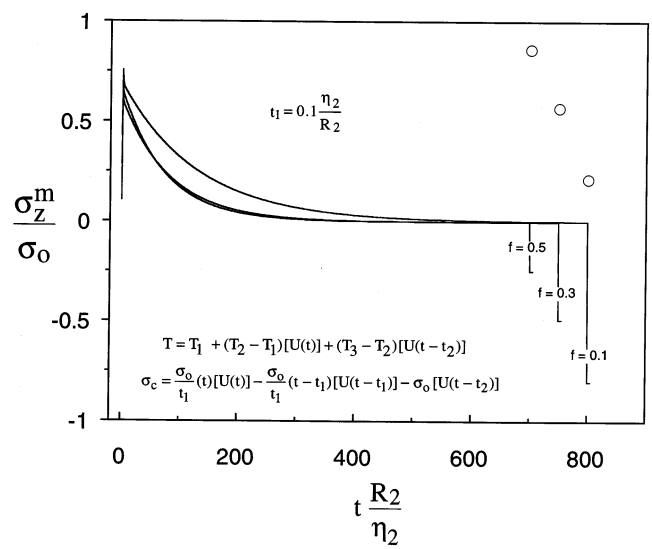

Fig. 9. Predicted evolution of the axial stress in the matrix when the model composite is subjected to the thermomechanical schedule shown in Fig. 7. The open circles indicate the state of residual stress that would exist in the matrix if the composite had simply been cooled from the stress-free fabrication temperature, T_1, down to the service temperature, T_3. The model predictions are shown for three values of the fiber volume concentration. Note that at the end of the treatment, the matrix is subjected to relatively large compressive residual stresses, and that its magnitude is inversely proportional to the fiber concentration.

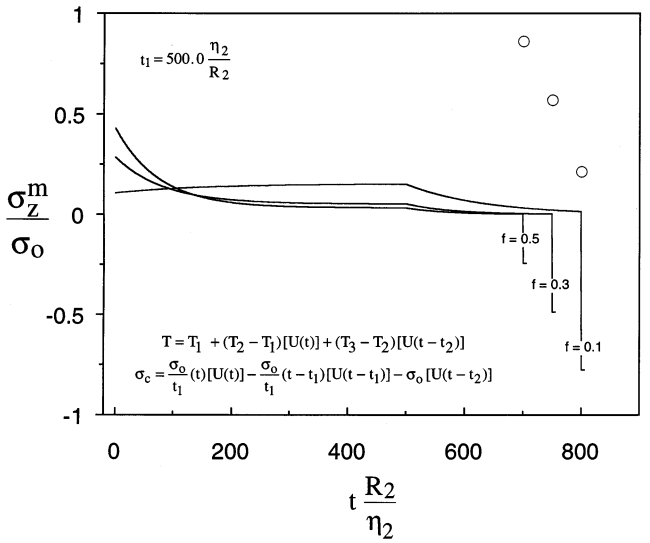

Fig. 10. Predicted evolution of the axial stress in the matrix when the model composite is subjected to the thermomechanical schedule shown schematically in Fig. 7. The results are similar to those in Fig. 9, but were obtained at a loading rate 5000 times slower.

are consistent with the experimental observations of Holmes et. al. in which matrix cracking was avoided by slowly loading the composite to the test stress [8]. Obviously, 'fast' and 'slow' loading will only be relative to the time scales associated with the creep behavior of a particular composite's constituents.

4. Discussion

Some of the implications of the results presented in Section 3 are obvious. For example, the successful applicability of the concept demonstrated here, to increase the matrix cracking stress of some brittle-matrix composites relies on the availability of fibers that are much more creep-resistant than the matrix, and that are strong enough to withstand the overloading conditions that will take place during the treatment and thereafter. It was shown that when complete matrix relaxation occurs, the stress in the fibers will be proportional to σ_0/f, so while it may be necessary to maximize the concentration of fibers in the loading direction to minimize fiber overloading, it may be desirable to minimize the fiber concentration to maximize the magnitude of the compressive residual stresses in the matrix. Therefore, a balance of these two factors will be necessary, but the optimum value of fiber concentration will depend primarily on the fiber properties.

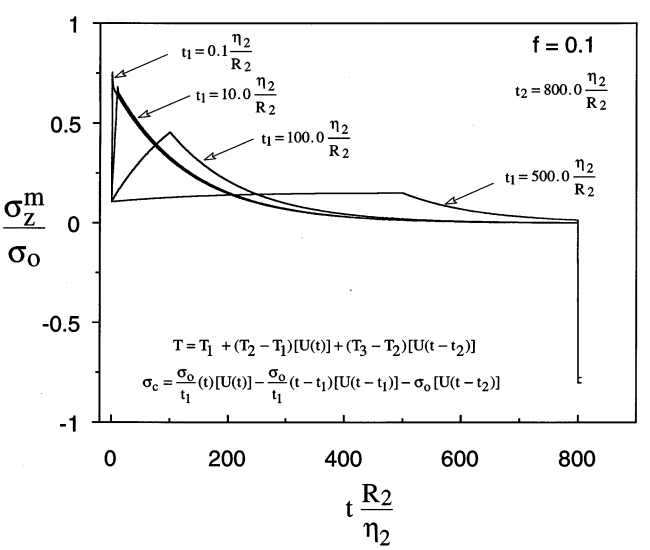

Fig. 11. Effect of the loading rate on the evolution of the axial stress in the matrix when the model composite is subjected to the thermomechanical schedule shown in Fig. 7. The results are presented for the case when $f = 0.1$. It can be observed that the maximum tensile stress which the matrix is subjected to increases with the loading rate.

In relation to the case of pre-stressed concrete where the concrete matrix is in a stress-free state while the reinforcements are being stressed, in the case modeled here the matrix is induced into a new stress-free state at a temperature different from the original stress free fabrication temperature, by stress redistribution. Otherwise the mechanisms are similar, i.e. once the load is removed (from the reinforcing bars in pre-stressed concrete, or from the composite in this case) it is through the elastic recovery (thermoelastic recovery in the case modeled here) of the reinforcing phases that the matrix is subjected to compressive stresses.

It must be pointed out that because the only driving force for the redistribution of stresses in the model composite considered in this paper is the creep deformation of the matrix, redistribution of internal stresses would occur even in the absence of externally applied stresses. In other words, a temperature decrease from the stress-free temperature T_1, to T_2, in the absence of externally applied stresses ($\sigma_c = 0$), would suffice to induce relaxation of internal stresses in the composite (i.e. annealing), as long as temperature T_2 is high enough to induce matrix creep. This effect was partly evident in Fig. 10, when it was observed that for $t < t_1$, and $f = 0.3$, and $f = 0.5$, the stress in the matrix decreases despite the fact that the stress in the composite continues to increase. However, although a simple thermal treatment in the absence of mechanical loading will change the stress-free temperature of the composite from T_1 to T_2, it would not produce the desired effect. The desired effect can only be accomplished by applying an external stress during the treatment, that would eventually be borne by the fibers as a result of the stress relaxation of the matrix, so when that load is removed from the composite, the matrix would be subjected to compressive residual stresses by the elastic recovery of the fibers.

An interesting prediction of this model is the relaxation of the normal interfacial stress as shown in Fig. 12. It must be pointed out that one of the interfacial mecha-

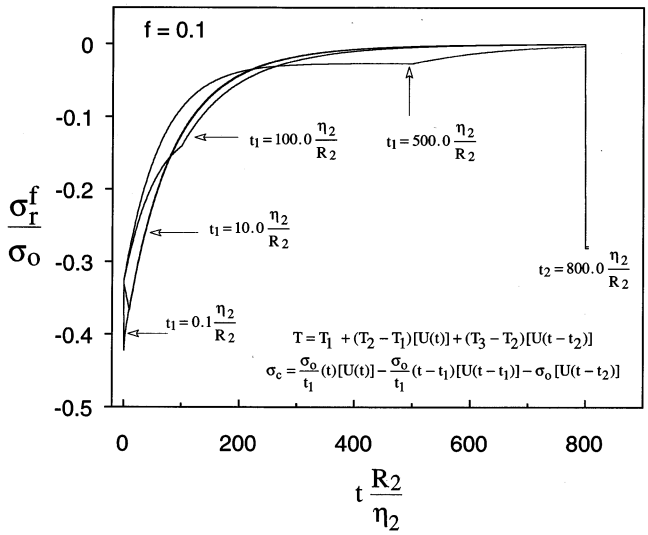

Fig. 12. Predicted evolution of the normal interfacial stress when the model composite is subjected to the thermomechanical schedule shown in Fig. 7.

nisms responsible for the tough behavior of CFCCs is fiber sliding, which at the same time, is influenced by the state of residual stresses at the fiber matrix interface. Therefore, the relaxation of the normal interfacial stress implies that the material may lose some of its 'composite-like' behavior. However, its behavior would then be dominated by the behavior of the fiber bundles.

5. Conclusions

A concept to increase the matrix cracking stress of some brittle-matrix composites was elaborated by formulating the stress analysis of a model unidirectional composite with linear viscoelastic phases. It was shown that it is possible to change substantially the state of residual stresses in such composite by means of a treatment that involves both thermal and mechanical loading, and that under certain conditions, it is possible to subject the matrix to large compressive stresses at the end of the treatment. Furthermore, it was found that the magnitude of the axial compressive residual stress induced in the matrix is inversely proportional to the concentration of fibers in the axial direction. It was also shown that such treatment results in the relaxation of the normal interfacial stress, which may affect micromechanical mechanisms responsible for the tough behavior of composites, such as fiber sliding. Because the induction of large compressive residual stresses in the matrix is achieved at the expense of fiber overloading, the practical viability of the concept demonstrated in this paper will depend on the availability of strong, creep-resistant fibers.

Acknowledgements

This research sponsored by the US Department of Energy, Assistant Secretary for Energy Efficiency and Renewable Energy, Office of Industrial Technologies, Industrial Energy Efficiency Division and Continuous Fiber Ceramic Composites Program, under contract DE-AC05-96OR22464 with Lockheed Martin Energy Research Corporation.

C.M. Russ, a sophomore at Washington University, St. Louis, MO, acknowledges the financial support from the Oak Ridge Institute for Science and Education, through the Professional Internship Program, to spend the summer of 1996 at ORNL. The authors are grateful to their colleagues Peter F. Tortorelli and Ellen Sun of Oak Ridge National Laboratory for reviewing the manuscript and for providing valuable comments.

References

[1] M.A. Karnitz, D.F. Craig, S.L. Richlen, Ceram. Bull. 70 (1991) 430–435.
[2] R.Y. Kim, N.J. Pagano, J. Am. Ceram. Soc. 74 (1991) 1082–1095.
[3] K.M. Prewo, J. Mater. Sci. 22 (1987) 2659–2701.
[4] E. Lara-Curzio, M.K. Ferber, R. Boisvert, A. Szweda, Ceram. Eng. Sci. 16 (1995) 341–349.
[5] A.G. Evans, F.W. Zok, J. Mater. Sci. 29 (1994) 3857–3896.
[6] Illustrated Science and Invention Encyclopedia, vol. 5, H.S. Stuttman, Publishers, Westport, CT 06889, 1992, pp. 603–604.
[7] E. Lara-Curzio, M.K. Ferber, Ceram. Eng. Sci. 16 (1995) 791–800.
[8] J.W. Holmes, Y. Park, J.W. Jones, J. Am. Ceram. Soc. 76 (1993) 1281–1293.
[9] J.W. Holmes, X. Wu, in: S.V. Nair, K. Jakus (Eds.), Elevated Temperature Mechanical Behavior of Ceramic Matrix Composites, Butterworth-Heinneman, London, 1994.
[10] E. Lara-Curzio, M.K. Ferber, Ceram. Eng. Sci. 15 (1994) 65–75.
[11] G.W. Scherer, S.M. Rekhson, J. Am. Ceram. Soc. 65 (1982) 352–360.
[12] E.H. Lee, Q. Appl. Math. 13 (1995) 183–190.
[13] W.N. Findley, J.S. Lai, K. Onaran, Creep and Relaxation of Nonlinear Viscoelastic Materials, Dover, New York, 1989.